Stretchability and Properties of Linear Low Density Polyethylene Blends for Biaxially Oriented Film

H.Uehara(1)*, K.Sakauchi(1), T.Kanai(2), T.Yamada(3)

(1) Okura Industrial Co.,Ltd

(2) Idemitsu Petrochemical Co.,Ltd

(3) Kanazawa University

*Corresponding author : h-uehara@okr-ind.co.jp

Abstract

In order to improve the stretchability of linear low density polyethylene (LLDPE) for double bubble tubular film (DBTF), the blending of LLDPEs have been investigated. Three linear low density polyethylenes of varying densities were blended, and several films were produced having different densites, molecular-weight distribution and composition distributions. The stretchability and properties of these films are investigated and the relationship between the stretchability and the material properties are also investigated. The material properties of LLDPE which have obtained better stretchability are reported on.

Furthermore, the stretchability of LLDPE by using the laboratory tenter biaxial stretcher and the double bubble tubular machine are compared. The prediction of the stretchability for the DBTF by using the laboratory tenter stretched film (LTSF) is reported, following up on the previous paper.

1. Introduction

The double bubble tubular polypropylene film is used to package stationary, groceries, foods and so on because of it's comparatively easier processability [1,2,3,4,5,6] and relatively cheaper resin cost. But recently, shrinkage film for this usage is required to have a superior appearance and shrinkage strength. The DBTF of LLDPE has both good shrinkage and high physical properties. For this reason the demand for DBTF of LLDPE has been increasing [7,8,9]. The deformation behavior, processability, and physical properties for the DBTF of LLDPE have been reported upon in the previous report [10]. LLDPE has a narrow stretchability range for the DBTF compared with polypropylene, hence blending of LLDPEs have been done in order to improve the stretchability and some patents [11,12,13] for

blending of LLDPEs have been applied for. Basic research such as phase behavior of blends with LLDPEs has been investigated by M.J. Hill and P.J. Barton [14,15]. But the biaxial stretchability changes in LLDPE blends and the reasons for such, have not been reported systematically. This paper will report on the relationship between the material properties and the biaxial stretchability, by using blends of three different density LLDPEs.

2. Experimental

2.1 Materials

The materials are LLDPE-A with a density of 0.920 g/cm^3 and a melt flow index of 1.0 g/10min, LLDPE-B with a density of 0.902 g/cm^3 and a melt flow index of 1.0 g/10min, and LLDPE-C with a density of 0.935 g/cm^3 and a melt flow index of 2.5 g/10min. Table 1 shows the material properties. Table 2 shows the blend ratios of materials and blended films' material properties. Figure 2(a) and 2(b) shows the measurement results of temperature rising elution fractionation (TREF) of the materials and each blended film.

2.2 Laboratory tenter biaxial stretcher

The laboratory tenter biaxial stretcher is type BIX-703 made by Iwamoto Seisakusho Co. which is the same machine as used in the previous report [10].

2.3 Double bubble tubular film machine

The double bubble tubular film machine which is shown in Figure 1, was also the same as in the former report. The DBTF line has been constructed by our company. The extruder is 65mm in diameter and made by Modern Machinery Company while the circular die is 180mm in diameter and made by Tomi Machinery Manufacturing Corporation. The take off tower, cooling water ring, infrared heater oven, and winder are all our own constructions. A torque measurement instrument SS201 made by Ono Sokki Co. in Japan is set between the take-up nip roll and driving motor, in order to calculate the stretching stress [16] from the stretching torque.

2.4 Experimental methods

2.4.1 Laboratory tenter stretched film

The test piece film for the laboratory tenter biaxial stretcher is the first stage bubble film from the

DBTF process. The stretch ratios are set at 5 in the machine direction (MD) and 5 in the transverse direction (TD). The thickness of this pre-stretched film is 300μm, and the after stretching film thickness is 12μm. Film size is a 95mm square, but with allowances for clipping, the effective stretching film size becomes a 70mm square. The heating time is 2 minutes, and the stretching speed is 30 mm/sec. The stretching temperature range is measured in 2 degree intervals, and also measured is the relationship between the stretch ratio and the stretching force under each stretching temperature. Further stretched film properties such as shrinkage, young's modulus and haze have been measured.

2.4.2 Double bubble tubular film

The MD and TD stretch ratios are 5. The thickness of the first bubble film is 375μm, and the film width is 235mm, while the final stretched film thickness is 15μm and film width is 1180mm. The output rate is 47 kg/h. The stretching ranges of the DBTFs are measured by using stretching torques. The stretching stresses are calculated from the stretching torques. The calculation theory of stretching stress is explained in detail in the former report [10]. The definition of the stretching range, is from the stress at the onset of bubble stability, to the stress just before bubble burst. With more than 5 Nm of stretching torque fluctuations, the bubble visibly moves, and as such is judged as bubble instability.
The film properties such as shrinkage, tear strength and haze at the conditions of maximum stretching stress and minimum stretching stress, are measured.

2.4.3 Evaluation methods of material and film properties

The material and film densities are measured by Accupyc 1330 made by Micromeritics Instrument Corporation. This equipment can measure the density faster than the density gradient tube method, while maintaining the same measurement accuracy. The melt index is measured by ASTM D 1238, and the melting point is measured by DSC (Seiko Instruments Inc. EXSTAR DSC6200R) method. The composition distribution is measured by the temperature rising elution fractionation (TREF) method using equipment made by Idemitsu Petrochemical Co.,Ltd [17]. The measuring conditions are as follows. The solvent is ortho-dichlorobenzen, the flow speed is 1.0ml/min, with the cooling temperature rate being 10 ℃/hr from 135℃ to 0℃ and the heating temperature rate, 40 ℃/hr from 0℃ to 135℃. An infrared detector is used and the TREF column size is Φ4.2mm×150mm, Chromosorb P are used as the fillers and the pour quantity is 0.5 ml with a concentration of 4 mg/ml. TREF relies on the crystallization and re-dissolution process to separate polymers having different degrees of branching.
The shrinkage, tear strength, and haze are measured by ASTM D 2732, ASTM D 1922 and ASTM D 1003 respectively. The refractive index of the stretched film is measured by Automatic Birefringence Analyzer KOBRA made by Oji Scientific Instruments Co.,Ltd [18] in Japan.

3. Results

3.1 Laboratory tenter stretched film

3.1.1 Stretchability

The stretching temperature ranges for each blended LLDPE film is shown in Table 3. The relationships between stretch ratio and stretching force within each stretching temperature range are shown in Figure 3(a)～3(c). The relationships between stretch ratio and stretching force of machine direction (MD) and transverse direction (TD) of LTSF have already been checked in the previous report. The data of MD and TD are almost the same, so only the MD data is shown. The stretching stresses are calculated from the stretching force, when the film is stretched to 5 times it's original size. The stretching stress and haze of the stretched films are also shown in Table 3. The stretching ranges of the DBTF are predicted from the haze and stretching stress as described in the former report. With an increase in film haze of more than 50 %, a too high stretching temperature is deemed, and is beyond the stable stretching range for the DBTF. In some cases it is difficult to judge only by haze, so the stretching stress below 7.5MPa is judged as an unstable range for the DBTF. In the previous report, the stable stretching stress range for the DBTF is from about 9 to 18 MPa, and the stretching stress of the LTSF that corresponds with it, is from about 7.5 MPa (MD) to 15.3 MPa (MD) which is about 85 % stretching stress of the DBTF. Hence, the stretching stress of 7.5Mpa was decided upon as the benchmark. As a result, the prediction of the stable bubble stretching range of DBTF is marked by hatching in Table 3.

Table 3 shows that when the very low density LLDPE-B is blended to LLDPE-A at a ratio of 15 % to 85 % respectively, the stretching temperature range is shifted 2 degrees lower than 100 % LLDPE-A. Furthermore, when the LLDPE-B is blended to LLDPE-A at a ratio of 30 % to 70 % respectively, the stretching temperature range is shifted 4 degrees lower than for 100 % LLDPE-A . This means that the average density decreases by blending low density LLDPE, and it results in a lower temperature stretching, however the heat resistance also decreases.

When the LLDPE-C is blended to LLDPE-A at a ratio of 15 % to 85 % respectively, the stretching temperature range is shifted 2 degrees higher than for LLDPE-A only. But when the LLDPE-C is blended to LLDPE-A at a ratio of 30 % to 70 % respectively, the stretching temperature range is narrower than for 100 % LLDPE-A. Hence it is considered that a too high density component inhibits the stretchability.

The blended film of LLDPE-A 70 %, LLDPE-B 15 %, and LLDPE-C 15 % has the widest stretching temperature range. This film density is the same as 100 % LLDPE-A film. This blended film's stretching force is lower than LLDPE-A film at the same stretching temperature shown in Figure 3. So a very low density LLDPE works to reduce the stretching force. This film contains about 24% high density component, to enable heat resistance and stretching in higher stretching temperature ranges.

Increasing the LLDPE-C content in the blend of LLDPE-A increases the average density, the yield load and stretching force as is shown in Figure 3 (C). As a result, stretchability at the lower stretching temperature becomes worse and the stretching temperature range narrows.

3.1.2 Relationship between stretchability and TREF, and DSC

The material properties such as composition distribution by TREF and the heat of fusion by DSC have been measured in order to analyze the stretchability. Figure 2(a) and 2(b) shows the composition distribution of the materials and blended films. When LLDPE-B is blended to LLDPE-A, the composition distribution becomes wider at lower temperatures resulting in a lowering of the high density component peak. When LLDPE-C is blended to LLDPE-A, the composition distribution becomes narrower and raises the high density component peak. When LLDPE-B (15%) and LLDPE-C (15%) are blended to LLDPE-A, the composition distribution becomes wider at lower temperatures and raises the peak of high density component. Further when LLDPE-B (30%) and LLDPE-C (30%) are blended to LLDPE-A, two distinct peaks emerge at approximately 73 ℃ and 97 ℃. It is considered that the high density component is associated with heat resistance and the stretching force, while the lower temperature component is associated with low temperature stretchability. The balance of these components is very important.

The relationship between the elution temperature and integral ratios of the melting component from the TREF results are shown in Figure 4. The relationship between the temperature ranges of a certain melting component integral ratio and the stretchability are investigated. The gradients (%／℃) of the total melting component from 40% to 70% (region A), almost all represented by straight lines, were correlated with the stretchability. The blended film density is also considered an important parameter to evaluate the stretchability of LLDPE. Figure 5 shows the relationship among film density, gradient (%／℃) of the region A in TREF and stretchability. Figure 6 shows the relationship among the film density, gradient (%／℃) of the region A in TREF and the stretchable temperature range that is considered to cause deterioration of the film transparency (haze). This deterioration of the film transparency, means that the film surface has melted and increased the crystallinity, resulting in bubble instability for the DBTF. Furthermore, the deterioration of the film transparency decreases the production value. Hence it is necessary to consider the deterioration of the film transparency of the LTSF, in evaluating the stretchability of the DBTF.

Figure 6 shows that a better stretchability range is from 2.0 to 3.0 (%／℃) of the gradient. It is considered that the wide temperature range of region A of the integral melting component allows for easier stretching, but too greater a temperature range is detrimental to the stretching. Because of the moderately wide composition distribution, the temperature range of the melting component necessary for the stretching is also wide, hence the stretching temperature range is also wide. However when there is too wide a composition distribution (shown in Figure 2(b)) at low temperature, the high density component does not melt. When the temperature is raised to the necessary high density

component stretching level, the lower density component will melt completely, creating an unstable bubble condition.

Figure 6 also shows that a film density from 0.915 g/cm^3 to 0.917 g/cm^3 is better for stretchability. It is considered that a density lower than 0.912 g/cm^3 is from a lack of stretching stress, and a density higher than 0.919 g/cm^3 has too much high density component preventing good stretchability.

Figure 7 shows the relationship between the temperature and integral ratio of melting components of DSC. The same analysis techniques of TREF were used. The result is shown in Figure 8, but the relationship between stretchability and gradient is not clear. The reason is considered as follows. The DSC method measured the heat of fusion only in film crystallization. The amorphous part in the film fulfils the important role for stretching. Hence, the DSC method is not good enough to evaluate the stretchability of LLDPE.

3.1.3 Film properties

The film properties of each stretched film at the lowest temperature are shown in Table 4. Figure 9, 10 and 11 show the relationships between average film density and properties such as shrinkage, haze and young's modulus. The shrinkage of films stretched at 116 ℃ are shown in Table 5.

Figure 9 shows that the shrink ability is better in the film that LLDPE-B is blended when compared to the film that LLDPE-B is not blended, especially at a 110 ℃ shrink temperature. The film densities of LLDPE-A(70)+LLDPE-B(15)+LLDPE-C(15) (No.3) and LLDPE-A are the same, but the shrink ability of No.3 is better than LLDPE-A, because No.3 has a lower temperature stretchability than LLDPE-A.

Figure 10 shows the relationship between the film density and haze. All films have excellent haze. In a higher density film, the haze becomes slightly worse, because of an increase in the crystalinity.

The relationship between the film density and young's modulus is shown in Figure 11 with an interesting trend being apparent. The young's modulus was strongly influenced by the film density when it was under 0.912 g/cm^3 and over 0.915 g/cm^3. Between a film density of 0.912 g/cm^3 and 0.915 g/cm^3, minimal change was observed in the Young's modulus

3.2 Double bubble tubular film

3.2.1 Stretchability

The stretching stress range of the DBTFs are shown in Table 6. The stretching stress range is wider for the lower stretching stress side with the blending of LLDPE-B, because the stretching force became lower in terms of the LTSF study. However the higher stretching stress side became narrower when only LLDPE-B is blended because of the decrease in the high density component. So, the No.1 film which LLDPE-B 30 % blended to LLDPE-A has a narrower stretching stress range than LLDPE-A

100 % film. The higher stretching stress side is extended by blending LLDPE-C, while the lower stretching stress side becomes narrow after blending LLDPE-C. Hence No.3 has a good balance and the widest stretching stress range. These results follow a similar pattern regarding the stretchability order of the LTSF.

Figure 12 shows the relationship among film density, gradient (%／°C) of the region A in the TREF and stretchability for the DBTF. This data shows that a better stretchability range is from 2.0 to 3.0 (% ／°C) of the gradient, and around 0.915 g/cm^3 of the film density. The sample No7 (LLDPE-A 40%+ LLDPE-B 30%+ LLDPE-C 30%) has a very narrow stretching stress range compared to other samples. Such a pattern displaying two peaks of composition distribution in Figure 2(b) (in other words under 2.0 %／°C gradient from 40 % to 70 % melting component of the total in TREF) results in a deterioration of the bubble stability for the DBTF. Comparing this result with those of the LTSF (Figure 5 and Figure 6), Figure 6 when considering the deterioration of film transparency, is more useful in the predictability of DBTF stretchability than Figure 5.

The stretching stress of the DBTF is greater than the LTSF, because of non-isothermal stretching. This has been reported in the previous paper [10].

3.2.2 Film properties

The film properties of the maximum stretching stress and the minimum stretching stress are shown in Table 7. When comparing a higher stretching stress film's properties with a lower stretching stress ones, they follow the same trends that have been reported previously. A higher stretching stress film has better shrink ability and stronger physical properties than a lower stretching stress film.

A higher stretching stress film has a better shrinkage balance and strength balance of MD and TD than lower stretching stress film. This is due to the higher stretching stress film being stretched less in MD in the pre-heater oven, and is stretched more simultaneously than the lower stretching stress film.

There are a few changes in haze in the DBTF, because the bubble became unstable in too high a temperature, which causes the haze to worsen by melting the bubble surface.

When it is compared between blending films, lower density film displays better shrink ability. The young's modulus was influenced by the film density. A higher film density results in greater young's modulus.

4 Conclusions

It is effective to blend the different density of LLDPEs, in order to improve the stretchability of LLDPE for DBTF. By blending, the composition distribution expands, and the stretchable temperature range becomes wider. The lower density part reduces the stretching stress and extends the stretching range for the lower stretching stress side, and the higher density part maintain a high stretching stress.

However there are two important points to improve the stretchability of LLDPE. First, is that the gradient (%／°C) from 40 % to 70 % melting component of the total in TREF is from 2.0 %／°C to 3.0 %／°C, and second is that the blended film density is not lower than 0.912 g/cm^3 , and not higher than 0.919 g/cm^3. When considering packaging film, film stiffness and tightness are general requirements, so even within this range, a higher film density is better.

This will be confirmed using another LLDPE in the next paper. When the density range of the evaluation film is extended, it will then be necessary to consider the rate of change of the stretching stress in relation to the change in the stretching temperature.

Predicting the stretchability of LLDPE for the DBTF using the data of the LTSF, taking into account the haze and the stretching stress, has become more reliable.

References

1. U.S.Patent 2,979,777(1961), Goldman,M.(DuPont)
2. U.S.Patent 3,510549(1970), Tsubosita,K.,Kano,T.(Kojin)
3. U.S.Patent 3,260,776(1966), Lindstrom,C.,(W.R.Grace)
4. U.S.Patent 3,300,555(1967), Bild,F.,Robinson,W.(ICI)
5. U.S.Patent 4,112,034(1978), Nash,J.L.,Polish,S.J.,Carrico,P.H.(General Electric)
6. U.S.Patent 4,156709(1979), Kazuo,K.,Toyoki,W.(Okura Industrial)
7. U.S.Patent 4,597,920(1986), Ralph,G..(DuPont)
8. U.S.Patent 5,904,964(1999), Douglas,J.(DuPont)
9. U.S.Patent 5,298,202(1994), Schirmer,H.(W.R.Grace)
10. Uehara,H., Sakauchi,K. (Okura), Kanai,T.(Idemitsu), Yamada,T. (Kanazawa univ.) Submit IPPS (2002)
11. U.S Patent 4,801,652 (1989), Mizutani,T.,Isozaki,H(Kohjin)
12. U.S Patent 3,663,662 (1972), Ostapchenko,J.,Williamsville(Du Pont)
13. U.S.Patent 5,589,561(1996), Barry,R.,Pellereau,B.(Dow chemical)
14. Hill,M.J.,Barton,P.J.(Physics Laboratory, University of Bristol) :POLYMER Vol.35 Number 9 (1994)
15. Hill,M.J.,Barton,P.J.(Physics Laboratory, University of Bristol) :POLYMER Vol.38 Number 8 (1997)
16. Kanai,T.,Campbell,G.A.:FILM PROCESSING 7.1,Hanser Publishers (1999)
17. Housaki,T.(Idemitsu Petrochemical) :Bunseki (Japanese) Sep. p.518 (2000)
18. Kiyokazu,S.(Oji Scientific Instruments) :Plastics age (Japanese) April p.154 (2000)

Table 1 Properties of Linear low density polyethylenes

		LLDPE-A	LLDPE-B	LLDPE-C
Density	g/cm^3	0.920	0.902	0.935
Melt Index	g/10min	1.0	1.0	2.5
Melting point	℃	121	100	124
M_W	—	120,200	95,700	86,000
M_N	—	37,900	48,900	32,600
M_V	—	102,600	87,900	75,800
M_Z	—	352,700	168,700	196,500
M_W/M_N	—	3.17	1.96	2.64
M_Z/M_W	—	2.93	1.76	2.29
M_Z/M_N	—	9.31	3.45	6.03

M_W : Weight average molecular weight M_V : Viscosity average molecular weight
M_N : Number average molecular weight M_Z : Z-average molecular weight

Table 2 Material properties of blended films

		1	2	3	4	5	6	7
LLDPE-A		70	85	85	100	85	70	40
LLDPE-B		30	15	15				30
LLDPE-C				15		15	30	30
Film density	g/cm^3	0.911	0.912	0.915	0.915	0.917	0.919	0.915
MI	g/10min	1.0	1.0	1.1	1.0	1.1	1.3	1.4
M_W		104500	112400	108000	120200	109900	107900	92000
M_N		36700	35700	34600	37900	35200	33100	34500
M_V		90500	95300	91700	102600	93600	91500	80700
M_Z		280200	356000	338900	352700	321800	328200	230100
M_W/M_N		2.84	3.16	3.12	3.17	3.12	3.26	2.67
M_Z/M_W		2.68	3.17	3.14	2.93	2.93	3.04	2.50
M_Z/M_N		7.63	10.0	9.80	9.31	9.15	9.93	6.67

Table 3 The relationship between stretching temperature and stretching stress and haze of the films stretched by laboratory biaxial stretcher

		1		2		3		4		5		6		7	
Material	LLDPE-A	70		85		70		100		85		70		40	
	LLDPE-B	30		15		15								30	
	LLDPE-C					15				15		30		30	
Item		haze	stress	haze	stress	haze	stress	haze	stress	haze	stress	haze	stress	haze	stress
unit		%	MPa	%	MPa	%	MPa	%	MPa	%	MPa	%	MPa	%	MPa
Stretching temperature ℃	106	broken													
	108	0.4	13.4	broken		broken									
	110	0.53	11.6	0.55	13.3	0.8	14.7	broken							
	112	0.60	9.2	0.75	11.3	0.8	12.8	0.90	14.3	broken				broken	
	114	0.93	7.5	0.80	9.1	0.9	11.1	0.80	11.0	1.2	13.1	broken		1.1	11.0
	116	1.3	5.7	1.2	7.2	0.9	8.5	1.3	9.5	1.2	10.6	1.4	12.6	1.3	8.6
	118	1.9	3.7	1.5	4.8	1.1	5.9	1.7	6.4	1.5	7.8	1.6	9.0	1.8	6.4
	120	Melt		2.3	3.3	1.7	4.2	2.6	4.6	1.8	5.4	1.8	6.9	2.6	4.2
	122			Melt		2.7	3.0	3.4	3.1	4.2	3.3	2.7	4.1	4.0	2.8
	124					Melt		Melt		Melt		Melt		Melt	

＊Hatched area is the prediction of the stable bubble stretching range of DBTF, when considering the deterioration of film transparency and stretching stress.

Table 4 Properties of films stretched at lowest stretchable temperature by laboratory biaxial stretcher

		1	2	3	4	5	6	7
Material LL-A		70 %	85 %	70 %	100 %	85 %	70 %	40 %
Material LL-B		30 %	15 %	15 %				30 %
Material LL-C				15 %		15 %	30 %	30 %
Thickness	μm	12						
Stretching temperature	℃	108	110	110	112	114	116	114
Young's modulus Kg/cm²	MD	2030	2550	2750	2860	3290	4520	2600
	TD	2080	2590	3050	2920	3620	4930	2600
Haze	%	0.4	0.4	0.8	0.8	0.9	1.3	1.1
Shrinkage % MD/TD	90℃	9/10	5/5	8/9	6/7	6/7	5/5	4/4
	100℃	21/22	16/16	15/16	14/15	12/14	9/10	9/10
	110℃	49/51	44/45	42/43	32/33	30/31	23/25	28/29
	120℃	73/71	70/69	73/70	72/70	74/71	64/64	65/63

Table 5 Shrink properties of LTSFs stretched at 116℃

		1	2	3	4	5	6	7
Materials	LLDPE-A	70 %	85 %	100 %	85 %	70 %	70 %	40 %
	LLDPE-B	30 %	15 %				15 %	30 %
	LLDPE-C				15 %	30 %	15 %	30 %
Shrinkage % MD/TD	90℃	5/5	5/5	5/5	5/5	5/5	7/7	3/3
	100℃	11/11	11/11	10/11	9/10	9/10	12/13	9/10
	110℃	28/28	28/28	27/28	24/24	23/25	29/30	19/20
	120℃	70/64	70/65	73/67	70/67	64/64	70/68	59/59

Table 6 Stretching stress range of the double bubble tubular films

		1	2	3	4	5
Material	—	A/B=70/30	A/B/C =70/15/15	A=100	A/C=70/30	A/B/C =40/30/30
Stretching torque Nm	min	33.3	33.3	39.1	42.8	60
	max	56.5	71.0	71.0	73.2	64
Stretching stress σMD MPa	**min**	**9.0**	**9.0**	**10.5**	**11.5**	**16.2**
	max	**15.2**	**19.1**	**19.1**	**19.7**	**17.3**
	R	**6.3**	**10.2**	**8.6**	**8.2**	**1.1**

Table 7 Properties of double bubble tubular films

		1	2	3	4	5	6	7	8	9	10
Material		LL-A 70% LL-B 30%		LL-A 70% LL-B 15% LL-C 15%		LL-A 100%		LL-A 70% LL-C 30%		LL-A 40% LL-B 30% LL-C 30%	
Thickness	μm	15									
Film density	g/cm³	0.911		0.915		0.915		0.919		0.915	
Stretching stress σMD	MPa	9.0	15.2	9.0	19.1	10.5	19.1	11.5	19.7	16.2	17.3
Young's modulus MD	MPa	-	230	-	320	-	320	-	450	-	310
Tear strength MD/TD	mN	150 /90	160 /140	130 /70	180 /140	130 /90	180 /140	70/50	150 /110	90/70	120 /100
Shrinkage MD/TD	%	12/19	17/22	10/15	13/17	7/13	10/15	7/11	8/13	10/16	12/18
		23/31	30/36	16/22	24/30	14/21	20/26	11/18	14/20	21/29	23/29
		52/58	58/63	36/43	48/53	35/47	48/52	24/31	31/35	41/48	46/50
		78/75	78/79	72/74	73/75	71/74	73/75	68/69	68/70	73/75	74/76

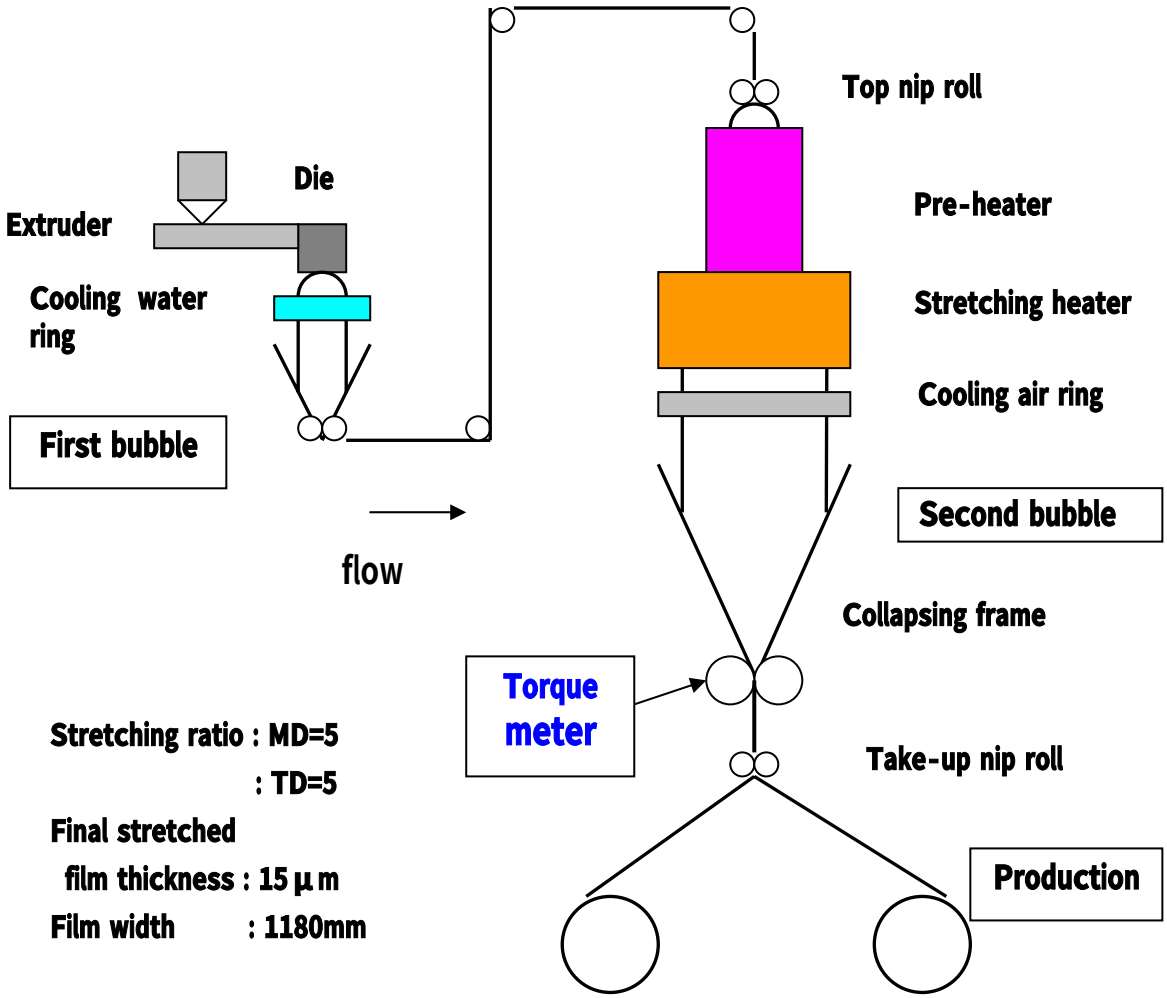

Figure 1 Schematic drawing of double bubble tubular film blowing process

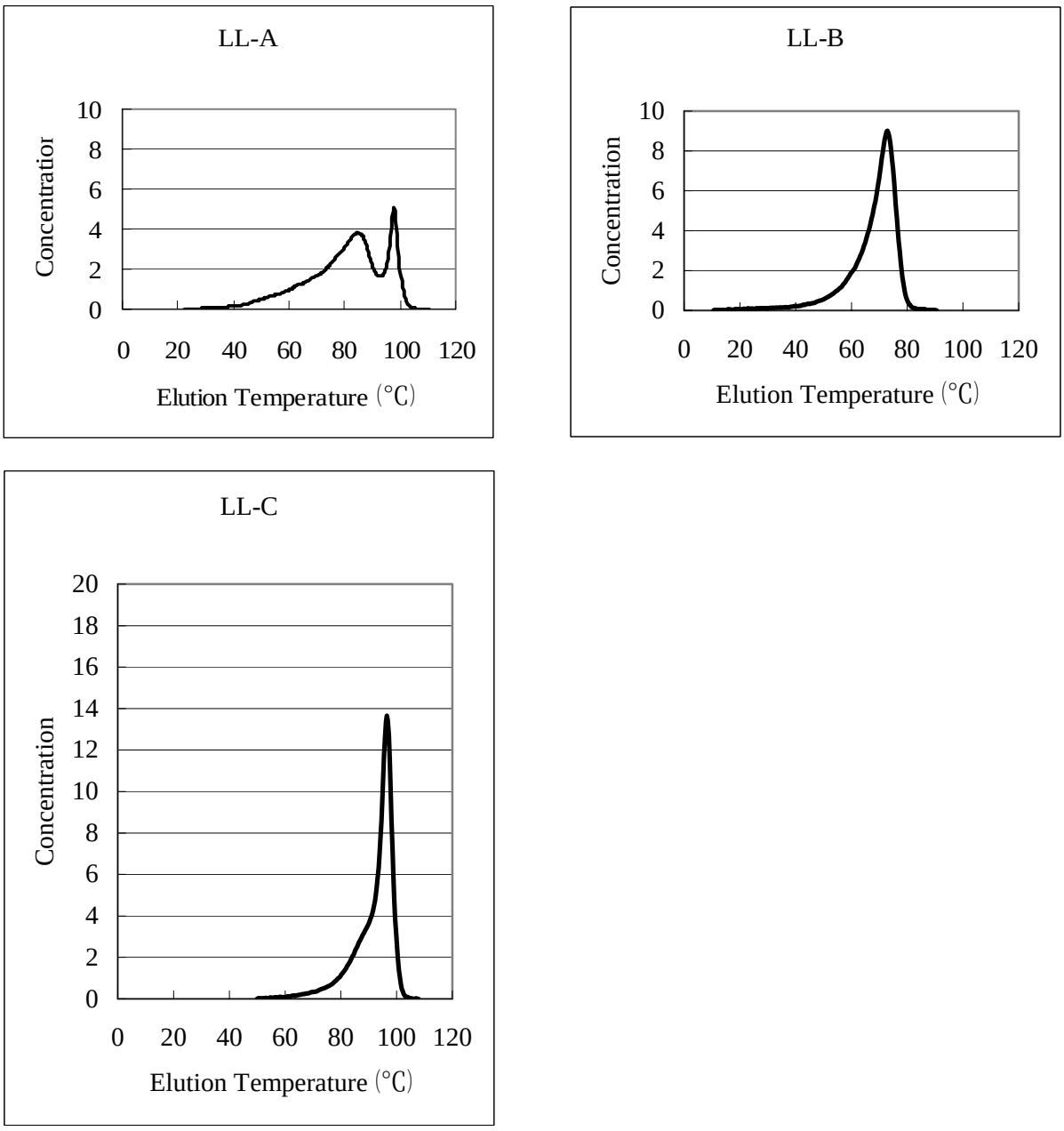

Figure 2 (a) Polymer separation results in TREF

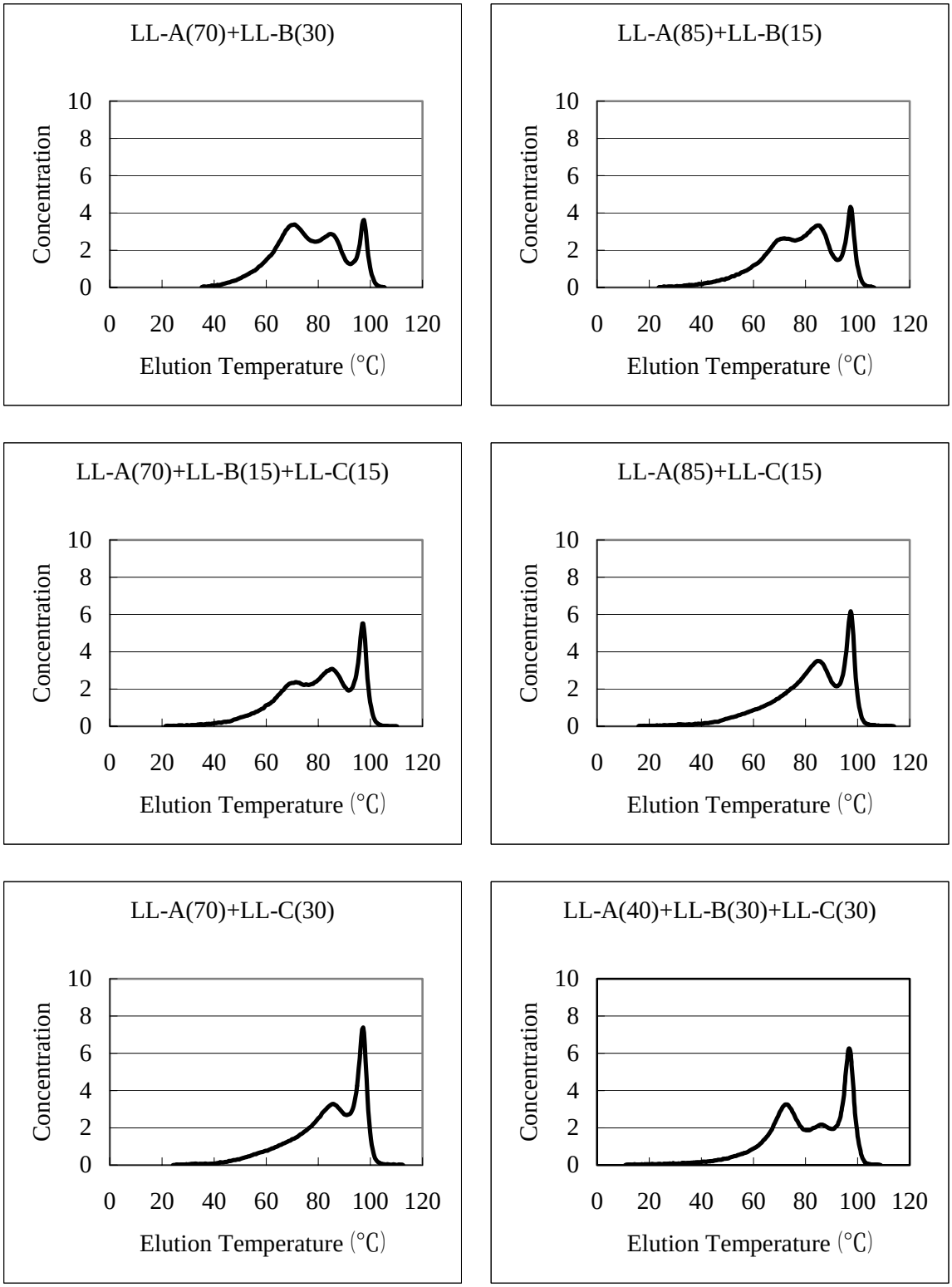

Figure 2 (b) Polymer separation results in TREF

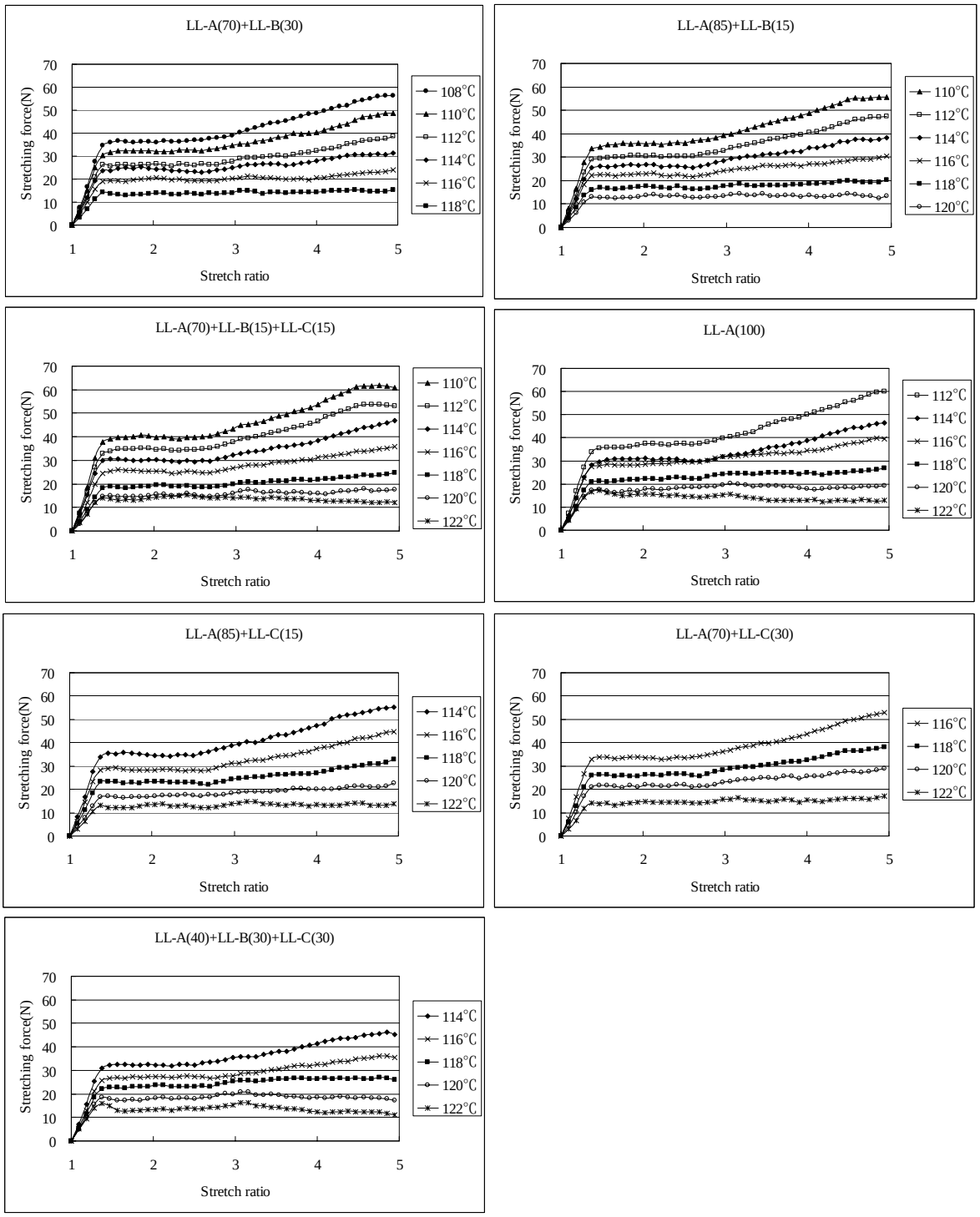

Figure 3　Relationship between stretch ratio and stretching force at each stretching temperature

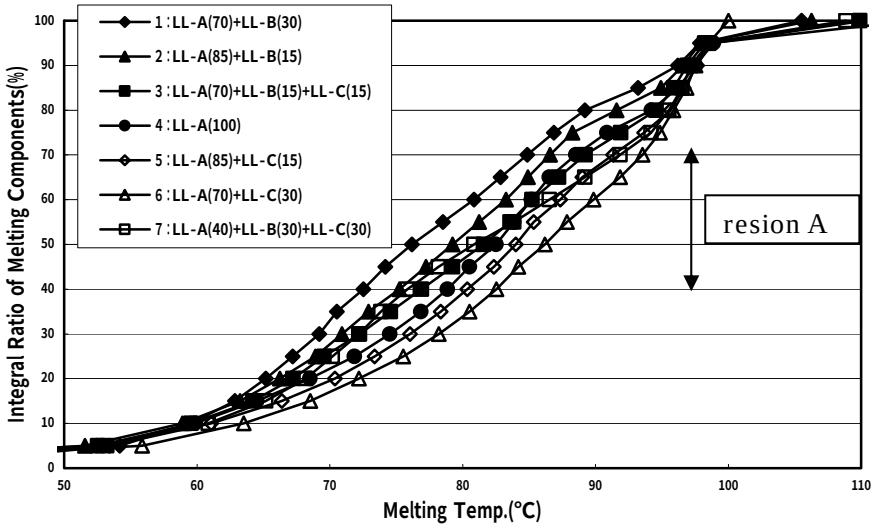

Figure 4 Integral ratio of melting component of TREF

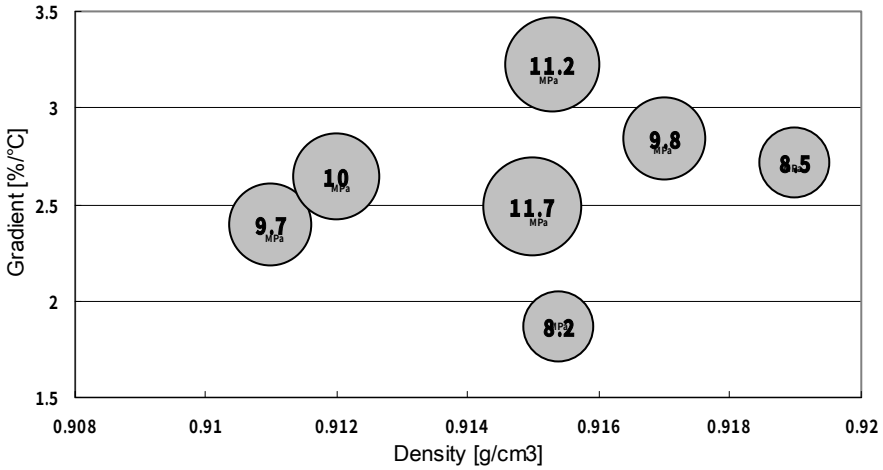

Figure 5 Relationship among density, gradient of TREF and stretching stress range of LTSF

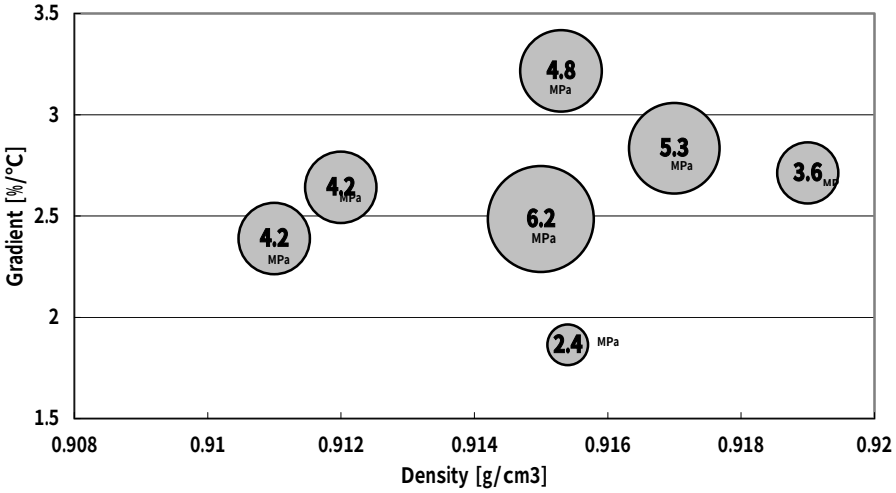

Figure 6 Relationship among film density, gradient of TREF and stretching stress range (considering transparency deterioration) of LTSF

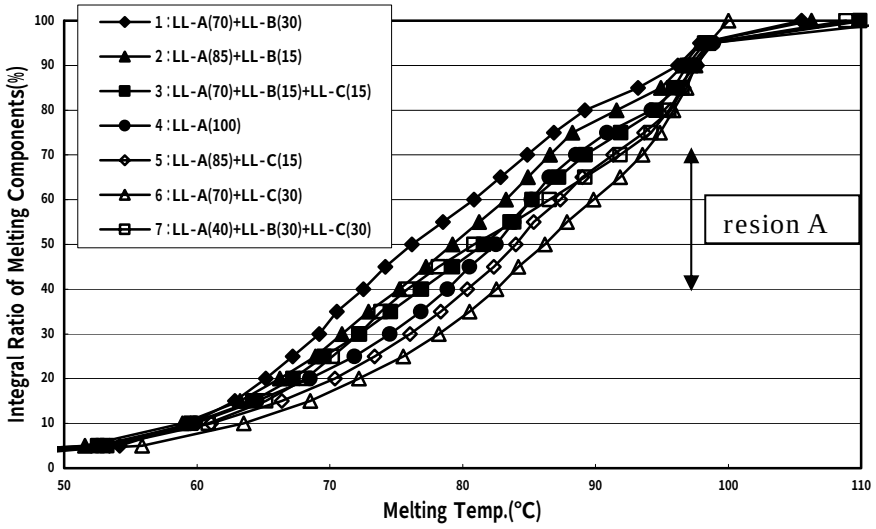

Figure 4 Integral ratio of melting component of TREF

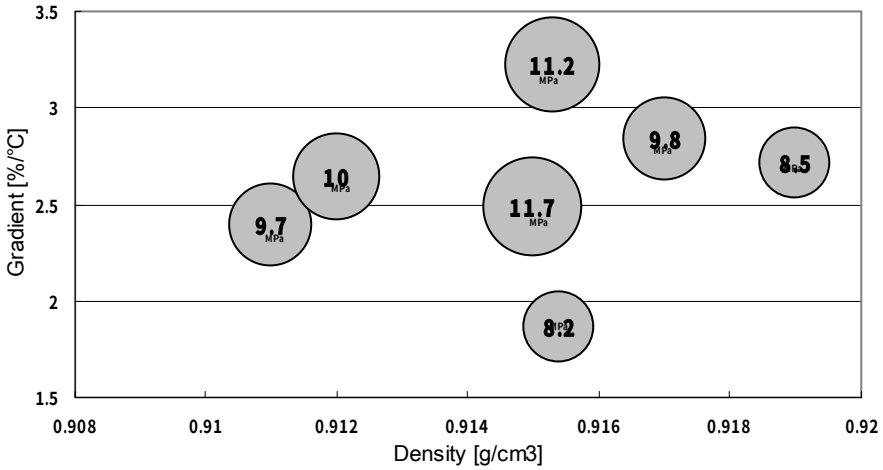

Figure 5 Relationship among density, gradient of TREF and stretching stress range of LTSF

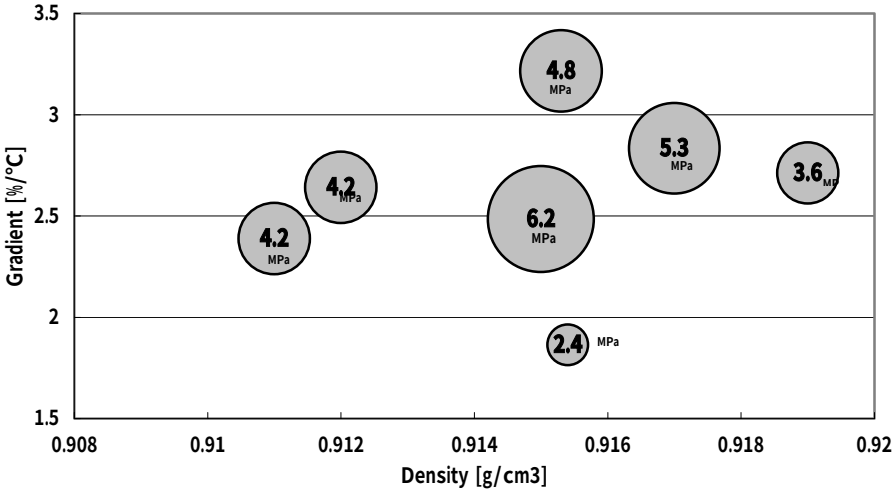

Figure 6 Relationship among film density, gradient of TREF and stretching stress range (considering transparency deterioration) of LTSF

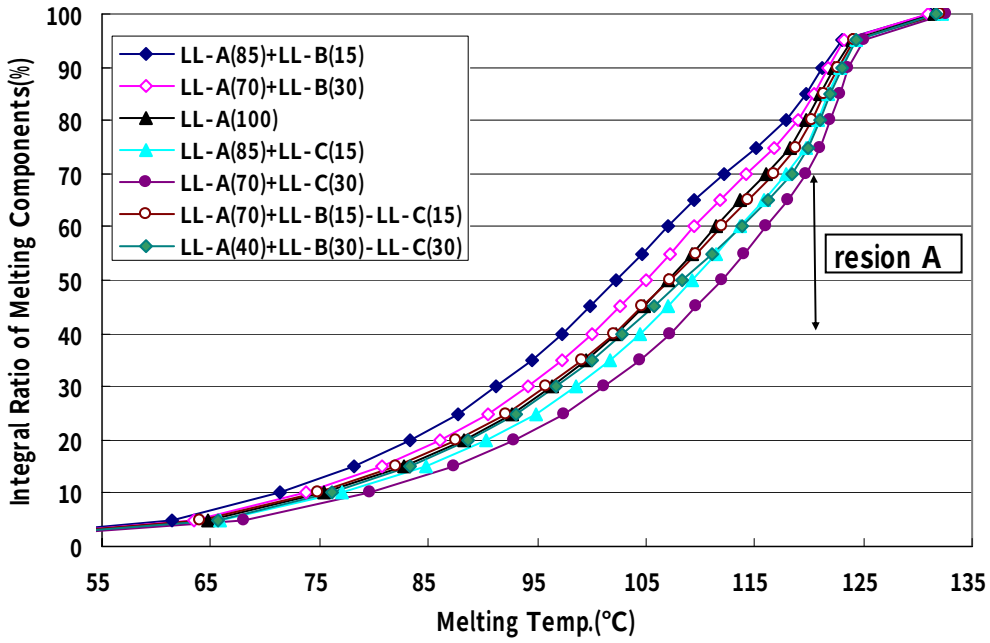

Figure 7 Integral ratio of melting components of DSC

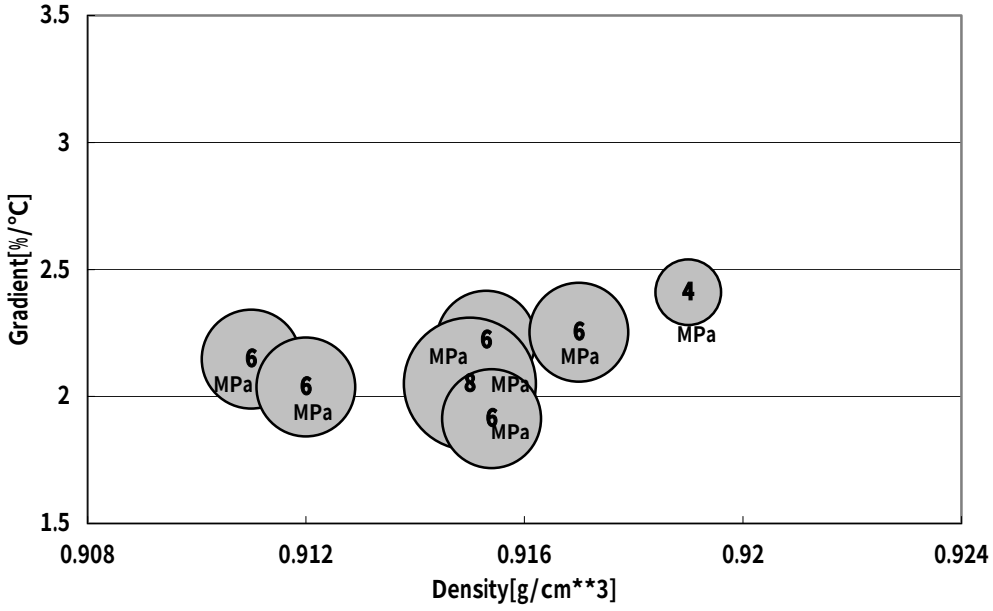

Figure 8 Relationship among film density, gradient of DSC and stretching stress range of LTSF

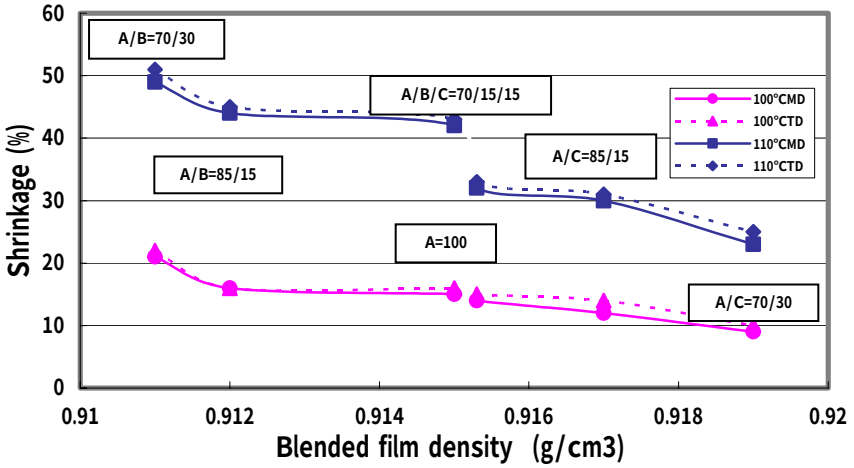

Figure 9 Relationship between blended film density and shrinkage of LTSF stretched at the lowest temperature

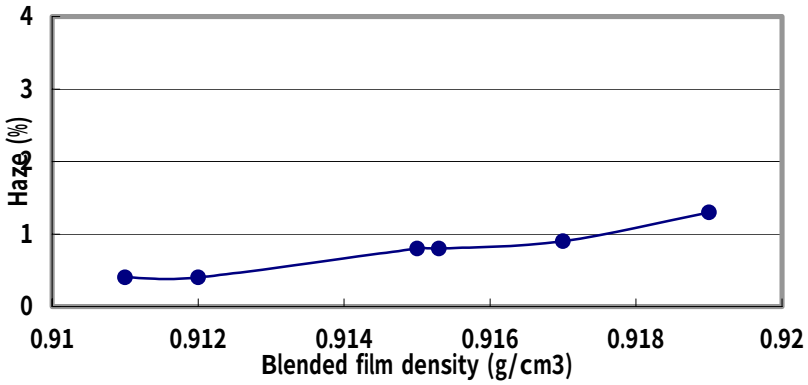

Figure 10 Relationship between blended film density and haze

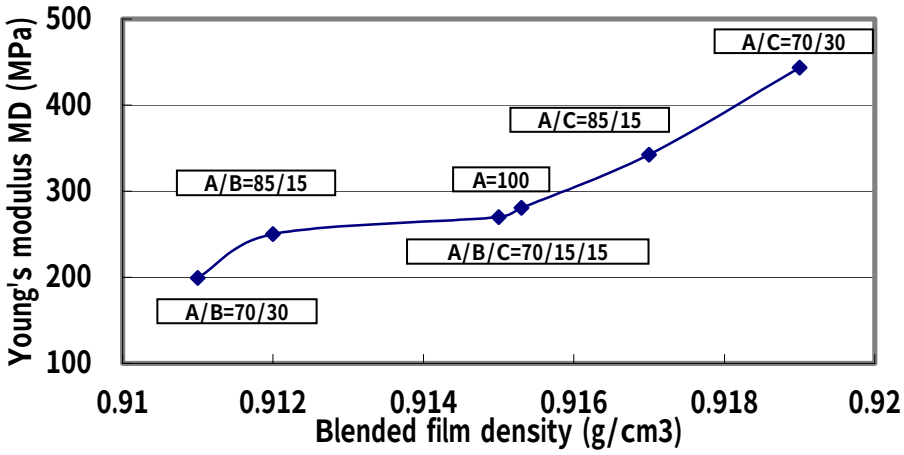

Figure 11 Relationship between blended film density and Young's modulus

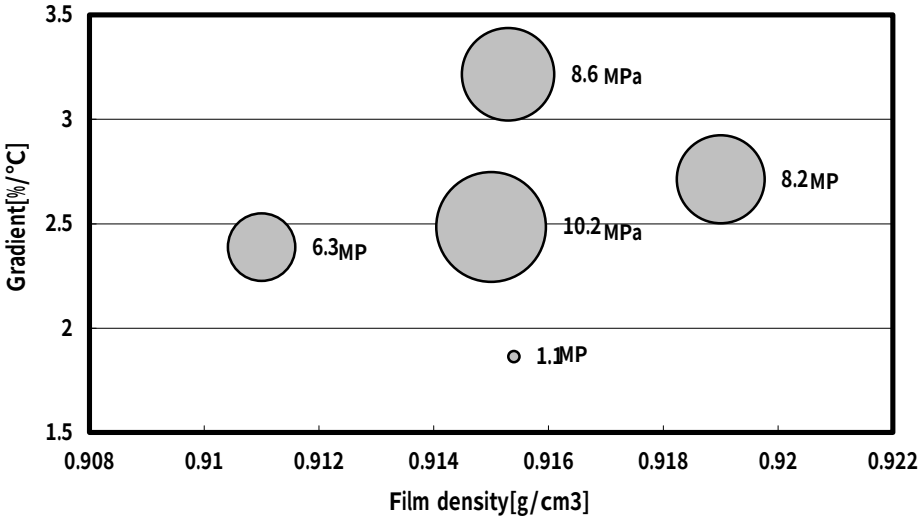

Figure 12 Relationship among film density, gradient of TREF and stretching stress range of DBTF